

Evaluation of Systemic and Mucosal Immune Responses Induced by a Nasal Powder Delivery System in Conjunction with an OVA Antigen in Cynomolgus Monkeys

Yusuke Torikai^{1,2}, Yuji Sasaki³, Keita Sasaki², Akifumi Kyuno², Shunji Haruta², and Akihide Tanimoto¹

Corresponding author: Yusuke Torikai

E-mail: torikai-yusuke@snbl.co.jp

Tel: +81 99 294 2600

Fax: +81 99 294 3619

Mailing address:

¹ Department of Molecular and Cellular Pathology, Kagoshima University Graduate School of Medical and Dental Sciences, 8-35-1 Sakuragaoka, Kagoshima, 850-8544, Japan

² R&D Department, TR Company, Shin Nippon Biomedical Laboratories, Ltd., 2438 Miyanoura, Kagoshima, 891-1394, Japan

³ Department of Pathology, Drug and Safety Research Laboratories, Shin Nippon Biomedical Laboratories, Ltd., 2438 Miyanoura, Kagoshima, 891-1394, Japan

Running title: A Powdery Nasal Formulation for Vaccines

Author's contributions:

Yusuke Torikai designed the study and wrote the initial draft of the manuscript. All other authors contributed to data collection and interpretation and critically reviewed the manuscript. All authors have approved the final version of the manuscript and agree to be accountable for all aspects of the work in ensuring that questions related to the accuracy or integrity of any part of the work are appropriately investigated and resolved.

ABSTRACT

An immune response for a nasal ovalbumin (OVA) powder formulation with an applied nasal delivery platform technology, consisting of a powdery nasal carrier and a device, was evaluated in monkeys with similar upper respiratory tracts and immune systems to those of humans, in order to assess the applicability to a vaccine antigen. Nasal distribution and retention studies using a 3D nasal cavity model and manganese-enhanced MRI were conducted by administering nasal dye and manganese powder formulations with the applied technology. Systemic and mucosal immune responses for the nasal OVA powder formulation were evaluated by determining serum IgG and nasal wash IgA antibody titers. The nasal dye and manganese powder formulations showed wider distribution and longer retention time than did a nasal liquid formulation. The nasal OVA powder formulation also showed comparable and higher antigen-specific IgG antibody titer to an injection and nasal liquid formulation, respectively. Furthermore, antigen-specific IgA antibody response was detected only for the nasal OVA powder formulation. The present study suggests that the technology, originally designed for drug absorption, is promising for nasal vaccines, enabling both a mucosal immunity response as the first line of defense and systemic immunity response as a second line of defense against infection.

KEY WORDS: Controlled delivery, Controlled release, Drug delivery system, Formulation, Immunogenicity, Mucoadhesive, Mucosal vaccination, Powder technology, Nasal drug delivery, Vaccine

ABBREVIATIONS:

BSA: Bovine serum albumin

CT: Computed tomography

HE: Hematoxylin and eosin

IgG: Immunoglobulin G

IgA: Immunoglobulin A

IM: Intramuscular

MAD: Mucosal atomization device

MALT: Mucosa-associated lymphoid tissue

MEMRI: Manganese-enhanced magnetic resonance imaging

Mn: Manganese

MRI: Magnetic resonance imaging

NALT: Nasopharyngeal-associated lymphoid tissue

OVA: Ovalbumin

PBS: Phosphate-buffered saline

SEM: Scanning electron microscopy

SIgA: Secretory immunoglobulin A

TMB: 3, 3', 5, 5'- tetramethylbenzidine

3D: Three dimensions

INTRODUCTION

In recent years, respiratory infections such as new strains of influenza, Middle East Respiratory Syndrome, and Severe Acute Respiratory Syndromes such as COVID-19 (a new coronavirus infection) have become major public health issues as the viruses have spread worldwide. As part of the preparations for the emergence of respiratory tract infections, a number of studies on techniques to powderize vaccine antigens, enabling cold-chain-free storage and distribution, have been reported.¹ Additionally, a number of studies on nasal vaccination as an alternative to conventional subcutaneous or intramuscular (IM) vaccination routes to defend against viral infection in the upper respiratory tract have been reported, and an attenuated influenza vaccine nasal spray (FluMist® and Nasovac®) is currently on the market.^{2, 3} The mucosal immunity achieved by nasal vaccination, which is mainly due to production of secretory immunoglobulin A (SIgA) as an immune response of nasopharyngeal-associated lymphoid tissue (NALT) and lymphoid tissues such as Waldeyer's tonsillar ring, has a crucial role in defending against viral infection in the upper respiratory tract.^{4, 5, 6} It has been reported that SIgA is also effective against mutated antigens, as it exhibits cross-protection.⁷ Therefore, a nasal vaccine is keenly anticipated to be developed as a pre-pandemic prophylactic against new strains of influenza as well as a defense against easily mutated antigens such as influenza antigen. However, since most research and development on nasal vaccines is intended for delivering vaccine antigens in a liquid form to the nasal cavity, there is a great need for nasal platform technologies that deliver a powder form against emerging respiratory viral infections due to their potential for cold-chain-free storage and distribution.

We have developed a proprietary delivery platform for nasal drug absorption, consisting of an inactive and highly safe nasal powder carrier with excellent affinity for the nasal mucosa and a nasal device that can deliver powder preparations widely and efficiently into the nasal cavity. In previous pharmacokinetic studies with cynomolgus monkeys, we demonstrated that the nasal delivery platform, in administering nasal drug powder formulations containing a low molecular weight drug, zolmitriptan, and a peptide, oxytocin, enabled rapid and high drug absorption.^{8, 9, 10} The nasal delivery platform, which was originally designed for nasal drug absorption, could be useful in enhancing immune response if the nasal vaccine powder formulation applied increases the chance of a vaccine antigen making contact with lymphoid tissues such as NALT and Waldeyer's tonsillar ring in the upper respiratory tract.

In the present study, in order to preliminarily assess the applicability of the nasal delivery platform to a vaccine antigen, the immune response of a nasal powder formulation containing ovalbumin (OVA), a model antigen, was evaluated using cynomolgus monkeys, which have similar nasal anatomy and nasal lymphoid

tissue to those of humans.

MATERIALS AND METHODS

Animals

Fourteen male *Macaca fascicularis* cynomolgus monkeys (purpose-bred, B-virus antibody negative; Shin Nippon Biomedical Laboratories, Ltd., Kagoshima, Japan), weighing between 2.9 to 6.3 kg, were used. All animal experiments were conducted with the approval of the Institutional Animal Care and Use Committees of Shin Nippon Biomedical Laboratories, Ltd. (Approval No. IACUC996-201), which is a fully The Association for Assessment and Accreditation of Laboratory Animal Care International (AAALAC)-certified facility.

Histopathology of Nasal Lymphatic Tissues

Histological examinations were conducted to identify the lymph tissues in the upper respiratory tract of monkeys. Two monkeys were euthanized after anesthetization with sodium pentobarbital solution (64.8 mg/mL, 0.4 mL/kg; Tokyo Chemical Industry Co., Ltd., Tokyo, Japan) into the cephalic vein, after which the upper respiratory tract mucosa was collected and fixed in 4% formaldehyde solution. For one of these monkeys, Harris hematoxylin staining of the upper respiratory tract mucosa, including the nasal cavity, was performed to visually observe the lymph tissue. For the other monkey, the fixed nasal cavity was divided into the nasal vestibule, respiratory, and olfactory regions, and the specimens were decalcified using Kalkitox (Wako Pure Chemical Industries, Osaka, Japan). After decalcification, the sections were paraffin-embedded, thinly sliced (50 μ m), and stained with HE.

Formulations

Red dye (new cocchine) was purchased from FUJIFILM Wako Pure Chemical Corporation (Osaka, Japan). Nasal Dye Liquid Formulation was prepared by dissolving 10 mg of the red dye in 1 mL of physiological saline for injection (Otsuka Pharmaceutical Factory, Inc., Tokushima, Japan). Nasal Dye Cellulose Powder Formulation was prepared by mortar-mixing the red dye with a cellulose carrier, a proprietary nasal powder carrier, of which the main component was a microcrystalline cellulose with a mean particle size of ≤ 50 μ m, a degree of polymerization range of 100 to 300, and a bulk density of ≤ 0.4 g/cm³ (Ceolus® PH grade, Asahi Kasei Corp., Tokyo, Japan) at a weight ratio of 1:24. Nasal Dye Trehalose Powder Formulation was prepared by mortar-mixing the red dye with trehalose dihydrate (FUJIFILM Wako Pure Chemical Corporation) at a weight ratio of 1:24. Manganese chloride tetrahydrate (MnCl₂·4H₂O) was purchased from Sigma-Aldrich Co. (St. Louis, MO).

Nasal Mn Liquid Formulation was prepared by dissolving 5 mg of $\text{MnCl}_2 \cdot 4\text{H}_2\text{O}$ in 10 mL of physiological saline for injection. Nasal Mn Cellulose Powder Formulation and Nasal Mn Trehalose Powder Formulation were prepared by mortar-mixing $\text{MnCl}_2 \cdot 4\text{H}_2\text{O}$ with the cellulose carrier and trehalose dihydrate, respectively, at a weight ratio of 0.1:25. OVA was purchased from Sigma-Aldrich Co. Nasal OVA Liquid Formulation was prepared by dissolving 10 mg of OVA in 2 mL of physiological saline for injection. Nasal OVA Cellulose Powder Formulation was prepared by mortar-mixing OVA with the cellulose carrier at a weight ratio of 1:49. IM OVA Injection was prepared by dissolving 10 mg of OVA in 5 mL of physiological saline.

Morphology and Particle Size of Powder Formulation

The morphology of each powder formulation was evaluated using a scanning electron microscope (TM3000, Hitachi High Technologies, Tokyo, Japan) at 15 kV accelerated voltage under a vacuum. The median particle size (D_{v50}) of each powder formulation was also measured using a laser diffraction particle size analyzer (Mastersizer 2000; Malvern Instruments Ltd., Malvern, UK) at an air pressure of 2 bars under dry condition. Additionally, morphologies and particle sizes for the microcrystalline cellulose, the main component of the cellulose carrier, and trehalose dihydrate, the carrier of the nasal trehalose powder formulations, were examined.

Nasal Delivery Device

The nasal powder formulations were delivered into a 3D monkey nasal cast or to monkeys using a Fit-lizer™ Type A for Non-Human Primates (hereafter, “nasal delivery device”; SNBL, Ltd., Kagoshima, Japan), a proprietary device, as shown in Figure 1. For each nasal powder formulation, a hydroxypropyl methylcellulose capsule (Qualicaps Co. Ltd., Nara, Japan) filled with a unit dose of the nasal powder formulation was loaded into the nasal delivery device, and the nasal powder formulation in the capsule was delivered by squeezing the pump of the device. For the nasal liquid formulation, a disposable syringe attached to a spray nozzle (Intranasal Mucosal Atomization Device [MAD], Teleflex Inc., Morrisville, NC) was filled with a unit dose of the nasal liquid formulation, which was delivered by depressing the plunger of the syringe.

Spray Characteristics of Powder and Liquid Formulations

The spray pattern and plume geometry of each nasal formulation which was delivered from the device were measured by the SprayVIEW® Measurement system (Proveris Scientific Corporation, Hudson, MA) equipped with the SprayVIEW automated nasal spray pump actuation system^{11, 12}. For spray characteristic measurements,

unit doses of nasal powder and liquid formulations were set as 25 mg and 100 μ L, respectively. All formulations were vertically emitted from the nasal delivery devices, perpendicular to the laser light. For spray pattern measurements, a horizontal laser sheet was positioned 3 cm above the device tip, and the spray pattern was imaged from above. For plume geometry measurements, the laser sheet was oriented vertically along the long axis of the nasal delivery device, and the plume was imaged from the side, directly above the device tip. All the images were captured at 500 frames/s. Three replicate measurements were conducted for each formulation in ambient conditions. The devices were weighed on an analytical balance (AB265-S/FACT, Mettler TOLEDO, Columbus, OH) before and after actuating to determine the delivered weight.

***In Vitro* Nasal Distribution Analysis with a 3D Nasal Cavity Model**

The 3D nasal cavity model was generated by a 3D printer using CT/MRI data of cynomolgus monkeys. Nasal Dye Cellulose Powder Formulation (25 mg/nostril), Nasal Dye Trehalose Powder Formulation (25 mg/nostril), and Nasal Dye Liquid Formulation (100 μ L/nostril) were delivered into the 3D nasal cavity model. Red dye distributed on the side of the nasal turbinates in the 3D nasal cavity model was visually observed by removing a section of the nasal septum from the 3D nasal cavity model.

Manganese-Enhanced Magnetic Resonance Imaging Analysis for Nasal Distribution and Nasal Retention

Manganese-enhanced magnetic resonance images for Mn^{2+} were acquired with a 3.0 Tesla, head-dedicated MRI scanner (MAGNETOM Allegra, Siemens, Erlangen, Germany) with a surface coil (Takashima Seisakusho Co., Ltd., Kanagawa, Japan). Monkeys were administered 25 mg of Nasal Mn Cellulose Powder Formulation, 25 mg of Nasal Mn Trehalose Powder Formulation, or 100 μ L of Nasal Mn Liquid Formulation into their right nostrils ($n = 1$ for each nasal formulation). For imaging, the monkeys were anesthetized with 1.5–2.5% isoflurane in a 0.3:0.7 mixture of $O_2:N_2$ before, and approximately 20 minutes and 3 hours after administering each nasal formulation. The monkeys were placed in a tailored bed equipped with a brain stereotaxic apparatus. Physiological conditions were monitored using breathing and temperature probes. Following a localizer scan, a T1 weighted image sequence (repetition time/echo time [TR/TE] = 1010/12 ms; voxel size = 0.47 mm \times 0.47 mm \times 2 mm, and flip angle = 60 degrees with fat saturation) and three dimensional magnetization-prepared rapid gradient echo sequences (TR/TE = 2120/3.93 ms; spatial resolution = 0.5 mm isotropic, and flip angle = 60 degrees with fat saturation) of the nostril–olfactory bulb were acquired. The images were analyzed using

OsiriX MD software (Pixmeo SARL, Bernex, Switzerland).

Nasal Immunizations

Nasal OVA Cellulose Powder Formulation and Nasal OVA Liquid Formulation were administered at doses of 25 mg/nostril (0.5 mg of OVA) and 100 μ L/nostril (0.5 mg of OVA), respectively, every two weeks for a total of three times into both nostrils of conscious monkeys (1 mg/body/time of OVA, $n = 3$ monkeys/group). IM OVA Injection was administered at a volume of 0.5 mL (1 mg/body/time of OVA) every two weeks for a total of three times in conscious monkeys ($n = 3$ monkeys/group). To collect nasal washes from the nasal cavities, 0.5 mL of sterile phosphate-buffered saline (PBS) was repeatedly infused into and recovered from one nostril five times under anesthesia with IM injection of ketamine hydrochloride (50 mg/mL, 0.2 mL/kg; Arevipharma GmbH, Radebeul, Germany) and aqueous medetomidine solution (1 mg/mL, 0.08 mL/kg; Domitor, Orion Corporation, Espoo, Finland). The final PBS nasal wash recovered from the nostril was used to assay SIgA antibodies.

Enzyme-Linked Immunosorbent Assay to Determine Antibody Titers

One hundred microliters of OVA solution (10 μ g/mL) was added to each well of a 96-well plate (Thermo Fisher Scientific Inc., Roskilde, Denmark) and incubated overnight at 4°C to solidify the contents. The plate was washed three times with PBS containing 0.05% w/v of Tween-20, and after adding 300 μ L of PBS containing 2% w/v of bovine serum albumin (BSA), the plate was left at ambient condition for 1 h to perform blocking. The plate was again washed three times as above, and the serum or nasal wash solutions were diluted stepwise, 2-fold with 2% w/v of BSA and PBS containing 0.05% w/v of Tween-20, after which the plate was incubated for 1 h at 37°C. Samples to be initially prepared were diluted 500-fold for serum samples and 5-fold for nasal wash solutions. After washing the plate three times, again as above, 100 μ L/well of horseradish peroxidase-conjugated goat anti-monkey immunoglobulin G (IgG, Nordic Mubio, Tilburg, Netherlands) or goat anti-monkey immunoglobulin A (IgA, Nordic Mubio) was added, and the plate was incubated for 1 h at 37°C. After washing the plate four times as described above, TMB substrate was added, and the color was developed at room temperature for 15 min before adding 2N H₂SO₄ to stop the reactions. Absorbance for each sample was measured at 450 nm of optical density using a plate reader (ST Sunrise Remote, TECAN, Grödig, Austria). Each antibody titer was calculated as the value obtained by adding three times the standard deviation to the mean absorbance of all the cases before administration, as a cut-off value. Titers less than 500 for the anti-OVA-IgG antibody or less than 5 for an anti-OVA-IgA antibody were assigned values of 250 and 2.5, respectively.

All data generated or analyzed during this study are included in this article.

Statistical Analysis

In spray characteristics, all pairwise comparisons between formulations were performed by Tukey's test for each parameter. IgG and IgA values were analyzed using generalized gamma models for each time point. Differences between results obtained for OVA IM Injection and Nasal OVA Cellulose Powder Formulation and for Nasal OVA Liquid Formulation and Nasal OVA Cellulose Powder Formulation were tested using SAS software (Release 9.4, SAS Institute Inc., Cary, NC) with $p < 0.05$ considered significant.

RESULTS

Localization of Nasal-Lymphatic Tissue

Visual observations of the upper respiratory tract mucosa after Harris hematoxylin staining in untreated monkeys confirmed that NALTs are widely distributed from the middle of the nasal cavity to the pharynx and Waldeyer's ring, which is surrounded by lymphoid tissues such as the pharyngeal tonsils, tubal tonsils, palatine tonsils, and lingual tonsils localized in the pharynx (Fig. 2B). Additionally, in HE staining of the nasal vestibular, respiratory, and olfactory regions, NALTs were observed in all nasal mucosal regions (Fig. 2C).

Morphology and Particle Size of Powder Formulation

Scanning electron microscopy (SEM) images for each powder formulation, the microcrystalline cellulose, and the trehalose dihydrate are shown in Fig. 3. The fibrous form and rough surface of the microcrystalline cellulose and cuboidal form and smooth surface of the trehalose dihydrate were observed in SEM images. The morphologies of the nasal cellulose and trehalose powder formulations observed in the SEM images were comparable to those of the microcrystalline cellulose and trehalose dihydrate, respectively.

As shown in Table 1, median particle sizes (Dv50) for each powder formulation, the microcrystalline cellulose, and the trehalose dihydrate were in the range of 16 to 20 μm . There were no marked differences in the Dv50 between the nasal cellulose powder formulations and microcrystalline cellulose, and the nasal trehalose powder formulations and trehalose dihydrate, respectively.

Spray Characteristics of Powder and Liquid Formulations

Table 2 shows the spray characteristics of all formulations used in the present study. Regardless of the type of nasal device or formulation, the ratio of delivered weight was at least 98%, and almost all formulations were confirmed to be emitted from the nasal devices. The nasal liquid formulation emitted by the MAD was confirmed to have wider spray spread characteristics compared with the nasal powder formulations emitted by the nasal delivery device, since the plume angle and spray pattern (area) of each nasal liquid formulation were markedly greater than those of each nasal powder formulation, respectively (over 1.5 and 2 times). Also, the nasal powder formulations with the trehalose carrier tended to have a greater plume angle and spray pattern than those with the cellulose carrier, with the exception of the Mn formulations.

Evaluation of *In Vitro* Nasal Distributions

In order to evaluate nasal distribution patterns for each nasal formulation, Nasal Dye Liquid Formulation, Nasal Dye Cellulose Powder Formulation, and Nasal Dye Trehalose Powder Formulation were delivered into the 3D monkey nasal cavity model (Fig. 4B-1 to 4B-3). In the coronal plane from the front of the nasal cavity model, compared with the nasal powder formulations, Nasal Dye Liquid Formulation was more widely distributed from the vertical direction through the lower turbinate to the middle turbinate and horizontal direction of the middle turbinate, corresponding to spray characteristics shown in Table 2. In the sagittal plane of the nasal cavity model, both nasal powder formulations were more widely distributed from the anterior region to the posterior region of the model compared with the Nasal Dye Liquid Formulation, which was distributed mainly in the anterior region of the model.

Evaluation of *in Vivo* Nasal Distributions

In order to evaluate nasal distribution patterns in monkeys for each nasal formulation, Nasal Mn Liquid Formulation, Nasal Mn Cellulose Powder Formulation, and Nasal Mn Trehalose Powder Formulation were administered into the right nostrils of conscious cynomolgus monkeys, and Mn-contrast MRI-T1-enhanced images of the head were captured (Fig. 5). The first image capture time point after administration was set at 20 minutes due to technical time requirements for anesthesia induction and imaging. Additionally, the images at 3 hours after administration were evaluated. For the Nasal Mn Liquid Formulation, fewer Mn²⁺ signals were observed in the upper area of the middle turbinate at 20 minutes after administration (Fig. 5B-1). The signal was not observed for Nasal Mn Liquid Formulation in the nasal cavity 3 hours after administration. For Nasal Mn Cellulose Powder Formulation and Nasal Mn Trehalose Powder Formulation, strong Mn²⁺ signals were observed widely in the upper nasal turbinate at 20 minutes after administration, corresponding with the results of *in vitro* nasal distribution studies of the 3D nasal cavity model (Fig. 5B-2 and 5B-3). The signals were also observed for both powder formulations in the nasal cavity 3 hours after administration. In particular, the image 3 hours after administering Nasal Mn Cellulose Powder Formulation showed stronger signals compared with the image 3 hours after administering Nasal Mn Trehalose Formulation.

Systemic and Mucosal Immune Responses after Administering Nasal OVA Formulations and IM OVA Injections

In order to evaluate the effects on immune responses of the cellulose carrier and nasal delivery device, anti-OVA IgG antibody titers in serum and anti-OVA IgA antibody titers in nasal washes after administering Nasal

OVA Cellulose Powder Formulation to cynomolgus monkeys were determined using ELISA (Fig. 6). Additionally, IM OVA Injection and Nasal OVA Liquid Formulation were evaluated as the comparison groups. For the group receiving IM OVA Injection, the anti-OVA IgG antibody titer significantly increased two weeks after the second dose (Day 28) and then further increased two weeks after the third dose (Day 43). For the group receiving Nasal OVA Cellulose Powder Formulation, the anti-OVA IgG antibody titer increased two weeks after the second dose (Day 28) and further increased to the same level as that of the group receiving the IM OVA Injection two weeks after the third dose (Day 43). For the group receiving Nasal OVA Liquid Formulation, however, the anti-OVA IgG antibody titer only slightly increased, even two weeks after the third dose (Day 43). For the group receiving Nasal OVA Cellulose Powder Formulation, the anti-OVA IgA antibody titer significantly increased two weeks after the second dose (Day 28) and further increased two weeks after the third dose (Day 43), whereas, for the other two groups, no increase in the anti-OVA IgA antibody titer was observed, even two weeks after the third dose (Day 43). Nasal OVA Cellulose Powder Formulation showed a comparable increase in the anti-OVA IgG antibody titer in the serum compared with IM OVA Injection and an increase in the anti-OVA IgA antibody titer in the nasal wash, which was not observed with IM OVA Injection or Nasal OVA Liquid Formulation.

DISCUSSION

In humans, the Waldeyer's ring is generally considered the main tissue associated with the immune system in the upper respiratory tract; additionally, it is thought that NALTs play important roles as well, since they have been reported to be widely distributed in the nasal cavities of young children.^{13, 14} Although many studies on nasal vaccination have been reported, most of these studies used rodents,^{15, 16} which have only NALT as the principal lymphoid tissue in the upper respiratory tract. However, monkeys have Waldeyer's rings as well as NALTs and also have a nasal anatomy similar to that of humans,¹⁷ and therefore are the most appropriate animal model for extrapolating mucosal immune responses in the upper respiratory tract to humans.

Considering the mechanism of mucosal immunity induction via lymphoid tissue in the upper respiratory tract, increased contact between an antigen and lymphoid tissue in the upper respiratory tract is readily predicted to induce an effective immune response. In the present studies with the 3D nasal cavity model and manganese-enhanced MRI (MEMRI), the nasal powder formulations showed wide distribution from the anterior region to the posterior region. In contrast, the nasal liquid formulations showed limited distribution in the nasal vestibule and lower nasal cavity area even though they showed a wider plume angle and spray area than those for the nasal powder formulations in the present spray characteristic studies. Thus, an obvious difference in distribution was observed between dosage forms. In both the *in vitro* and *in vivo* nasal distribution evaluations, the nasal liquid formulation showed wide distribution from the lower turbinate to the middle turbinate in the coronal plane. However, in the sagittal plane, the nasal liquid formulation showed limited distribution in the anterior region compared that of the nasal powder formulation. These results suggest that the liquid formulations are not effective to widely distribute from the anterior region to the posterior region of the nasal cavity due to obstruction by the middle turbinate, which is notably overhung in the nasal cavity. Additionally, these results suggest that the powder formulations are easy to widely distribute from the anterior region to the posterior region of the nasal cavity, possibly by scattering immediately after impacting with the overhanging middle turbinate. The inconsistency between the wide plume angle and the nasal distribution limited in the anterior region of the nasal cavity for the nasal liquid formulations may be due to less scattering after impacting with the middle turbinate, and/or less impelling force to reach the posterior region of the nasal cavity resulting from a high air resistance with the wide plume angle.

The MEMRI images for the nasal cavity captured 20 minutes after dosing showed significant Mn²⁺ signals for the nasal powder formulations in contrast to the low Mn²⁺ signals for the Nasal Mn Liquid Formulation. Other *in vivo* PET imaging studies evaluating nasal distribution after dosing nasal liquid formulations were reported to

have retained an amount of the nasal liquid formulation in the nasal cavity even 30 minutes after administration.^{18, 19} Low Mn^{2+} signals for the Nasal Mn Liquid Formulation in the present MEMRI imaging study captured 20 minutes after dosing were probably due to a low detection sensitivity for the Mn^{2+} signal in the MEMRI imaging. However, the difference in the Mn^{2+} signal level 20 minutes after dosing between the Nasal Mn Liquid Formulation and the nasal Mn powder formulations was obvious. Also, the MEMRI images for the nasal cavity captured 3 hours after dosing showed a higher Mn^{2+} signal for the Nasal Mn Cellulose Powder Formulation when compared with the Nasal Mn Trehalose Powder Formulation, possibly due to high mucoc-affinitive characteristics of the cellulose carrier. These results of MEMRI suggest that the Nasal Mn Cellulose Powder Formulation showed a longer retention time in the nasal cavity when compared with other formulations. The effect of Nasal OVA Cellulose Powder Formulation containing OVA, a model antigen in the immune response, was evaluated in the present study. Nasal OVA Cellulose Powder Formulation showed a comparable increase in the anti-OVA IgG antibody titer in the serum to that observed with IM OVA Injection and significantly increased the anti-OVA IgA antibody titer in the nasal wash. In contrast, no increases in anti-OVA IgA antibody titer were observed for IM OVA Injection or Nasal OVA Liquid Formulation. Antigen-specific IgG antibodies in the serum and antigen-specific IgA antibodies in the nasal mucosa are produced by B cells stimulated by follicular T cells of the germinal center in the lamina propria of mucosa-associated lymphoid tissue (MALT) such as NALT and the tonsils after antigen presentation.^{20, 21} The polymer poly-Ig receptor (pIgR) binds to IgA antibodies and is taken up by the epithelial cell layer above the lamina propria, moves across the epithelial cells, and is secreted (SIgA).^{22, 23} It is considered that the Nasal OVA Cellulose Powder Formulation, having characteristics of wide nasal distribution and longer nasal retention time, contributed to increased contact of OVA with MALT, and enhanced antigen presentation and differentiation of IgG and IgA-positive plasma cells, resulting in increasing both anti-OVA IgG antibody titer in the serum and anti-OVA IgA antibody titer in the nasal washes. Also, it was observed that for a dose group of the Nasal OVA Cellulose Powder Formulation that an increase in anti-OVA IgA antibody titer in the nasal wash was delayed for approximately 2 weeks in comparison with the increase in anti-OVA IgG antibody titer in serum. This was considered to be due to polymerization of the anti-OVA IgA antibodies and subsequent secretion into the lamina propria.

Other studies on nasal vaccines with adjuvants such as monophosphoryl lipid A and CpG oligodeoxynucleotides to stimulate the innate immunity of Toll-like and other receptors, have been reported.²⁴ However, the use of adjuvants is often accompanied by safety issues.²⁵ Therefore, the approach in the present study, to distribute a vaccine antigen widely and extend the retention time in the nasal cavity without any adjuvants, is very useful in

enhancing immune responses efficiently and safely. Furthermore, since the nasal delivery platform technology used in the present study is designed for powdered forms, the system possibly contributes to storage of nasal vaccines at room temperature in combination with other technologies to stabilize powdered antigens (e.g., powderization with disaccharides).²⁶ Further research and development on nasal vaccine delivery technology enabling needle-free, enhanced immune response and cold-chain-free handling is highly anticipated, particularly for pandemic vaccine application, to efficiently and safely defend against emerging respiratory tract infections.

CONCLUSIONS

In the present study, the effect on the immune response of Nasal OVA Cellulose Powder Formulation containing OVA, delivered by a nasal delivery platform technology consisting of a powder carrier and a delivery device, was evaluated in cynomolgus monkeys. Nasal OVA Cellulose Powder Formulation showed a comparable increase in anti-OVA IgG antibody titer in serum as that with IM OVA Injection and an increase in the anti-OVA IgA antibody titer in the nasal wash, which was not observed with IM OVA Injection or Nasal OVA Liquid Formulation. These results suggest that the nasal delivery platform technology which was originally designed for nasal drug absorption is also promising for nasal vaccines enabling both the mucosal immunity response as a first line of defense and the systemic immunity response as a second line of defense against infection.

ACKNOWLEDGMENTS

All studies were conducted at Shin Nippon Biomedical Laboratories, Ltd. We are thankful to Mr. Takanori Sugimoto and Ms. Nami Yasuda of Shin Nippon Biomedical Laboratories, Ltd. for providing expertise that greatly assisted the research.

COMPLIANCE WITH ETHICAL STANDARDS

RESEARCH INVOLVING ANIMALS

All animal experiments were conducted with the approval of the Institutional Animal Care and Use Committees of Shin Nippon Biomedical Laboratories, Ltd. (Approval No. IACUC996-201), which is a fully AAALAC-certified facility.

CONFLICT OF INTEREST:

This study was funded by Shin-Nippon Biomedical Laboratories, Ltd (SNBL). Yusuke Torikai, Keita Sasaki, Yuji Sasaki, Akifumi Kyuno and Shunij Haruta are employees of SNBL.

REFERENCES

1. Tomar J, Born PA, Frijlink HW, Hinrichs WLJ. Dry influenza vaccines: towards a stable, effective and convenient alternative to conventional parenteral influenza vaccination. *Expert Rev Vaccines*. 2016;15(11):1431–1447.
2. Carter NJ, Curran MP. Live attenuated influenza vaccine (Flumist®; Fluenz™): a review of its use in the prevention of seasonal influenza in children and adults. *Drugs* 2011;71(12):1592–1622.
3. Kulkarni PS, Raut SK, Dhere RM. A post-marketing surveillance study of a human live-virus pandemic influenza A (H1N1) vaccine (Nasovac®) in India. *Human Vaccines & Immunotherapeutics* 2013;9(1):122-124.
4. Turula H, Wobus CE. The role of polymeric immunoglobulin receptor and secretory immunoglobulins during mucosal infection and immunity. *Viruses* 2018;10(5):237.
5. Zuercher AW, Coffine S, Thurnheer C, Fundova P, Cebra JJ. Nasal-associated lymphoid tissue is a mucosal inductive site for virus-specific humoral and cellular immune responses. *J Immunol*. 2002;168:1796–1803.
6. Wu HY, Nguyen HH, Russell MW. Nasal lymphoid tissue (NALT) as a mucosal immune inductive site. *Scand J Immunol* 1997;46:506-513.
7. Saito S, Sano K, Suzuki T, Ainai A, Taga Y, Ueno T, Tabata K, Saito K, Wada Y, Ohara Y, Takeyama H, Odagiri T, Kageyama T, Ogawa-Goto K, Multihartina P, Setiawaty V, Pangesti KNA, Hasegawa H. IgA tetramerization improves target breadth but not peak potency of functionality of anti-influenza virus broadly neutralizing antibody. *PLoS Pathog*. 2019;15(1):e1007427.
8. Akiyoshi Y, Haruta S. Pharmacokinetic analysis of absorption characteristics of a novel nasal zolmitriptan powder formulation in monkeys. 45th Controlled Release Society Annual Meeting, July 22–24, 2018, New York, USA.
9. Milewski M, Goodey A, Lee D, Rimmer E, Saklatvala R, Koyama S, Iwashima M, Haruta S. Rapid absorption of dry-powder intranasal oxytocin. *Pharma Res*. 2016;33(8):1936–1944.
10. Haruta S. Achieving the potential of nasal drug delivery. *ONdrugDelivery Magazine*. April 2012, Issue No 37;4-6.
11. Chauhan H. Addressing the challenges in nasal device testing: Evaluation of pump performance. Proveris Scientific White Paper. Proveris Scientific Corporation, 2018 November.
12. Liao L, Chauhan H, Newcomb A, L'Ecuyer T, Cordero SN, Leveille C. Spray pattern: A rapid and sensitive

early development tool for respiratory drug products. Proveris Scientific White Paper. Proveris Scientific Corporation, 2017 October.

13. Debertin AS, Tschernig T, Tonjes H, Kleemann WJ, Troger HD, Pabst R. Nasal-associated lymphoid tissue (NALT): frequency and localization in young children. *Clin Exp Immunol* 2003;134(3):503–507.
14. Harkema JR, Carey SA, Wagner JG. The nose revisited: a brief review of the comparative structure, function, and toxicologic pathology of the nasal epithelium. *Toxicol Pathol*. 2006;34(3):252–269.
15. Rowell J, Lo CY, Price GE, Mispion JA, Crim RL, Jayanti P, Beeler J, Epstein SL. The effect of respiratory viruses on immunogenicity and protection induced by a candidate universal influenza vaccine in mice. *PLoS ONE*. 2019;14(4):e0215321.
16. Huang J, Garmise RJ, Crowder TM, Mar K, Hwang CR, Hickey AJ, Mikszta JA, Sullivan VJ. A novel dry powder influenza vaccine and intranasal delivery technology: induction of systemic and mucosal immune responses in rats. *Vaccine*. 2014;23(6):794–801.
17. Pabst R. Mucosal vaccination by the intranasal route. Nose-associated lymphoid tissue (NALT) – structure, function and species differences. *Vaccine*. 2015;33(36):4406–4413.
18. Saito S, Ainai A, Suzuki T, Harada N, Ami Y, Yuki Y, Takeyama H, Kiyono H, Tsukada H, Hasegawa H. The effect of mucoadhesive excipient on the nasal retention time of and the antibody responses induced by an intranasal influenza vaccine. *Vaccine*. 2016;34(9):1201-1207.
19. Yuki Y, Nochi T, Harada N, Katakai Y, Shibata H, Mejima M, Kohda T, Tokuhara D, Kurokawa S, Takahashi Y, Ono F, Kozaki S, Terao K, Tsukada H, Kiyono H. In vivo molecular imaging analysis of a nasal vaccine that induces protective immunity against botulism in nonhuman primates. *J Immunol*. 2010;185(9):5436–5443.
20. Brandtzaeg P. Transport models for secretory IgA and secretory IgM. *Clin Exp Immunol*. 1981;44(2):221–232.
21. Ueno H, Banchereau J, Vinuesa CG. Pathophysiology of T follicular helper cells in humans and mice. *Nat Immunol*. 2015;16(2):142–152.
22. Tamura S-I, Ainai A, Suzuki T, Kurata T, Hasegawa H. Intranasal inactivated influenza vaccines: a reasonable approach to improve the efficacy of influenza vaccine? *Jpn J Infect Dis*. 2016;69(3):165–179.
23. Shikina T, Hiroi T, Iwatani K, Jang MH, Fukuyama S, Tamura M, Kubo T, Ishikawa H, Kiyono H. IgA class switch occurs in the organized nasopharynx- and gut-associated lymphoid tissue, but not in the diffuse lamina propria of airways and gut. *J Immunol*. 2004;172(10):6259–6264.

24. Takaki H, Ichimiya S, Matsumoto M, Seya T. Mucosal immune response in nasal-associated lymphoid tissue upon intranasal administration by adjuvants. *J Innate Immun.* 2018;10(5–6):515–521.
25. Mutsch M, Zhou W, Rhodes P, Bopp M, Chen RT, Linder T, Splyr C, Steffen R. Use of the inactivated intranasal influenza vaccine and the risk of Bell's palsy in Switzerland. *N Engl J Med.* 2004;350(9):896–903.
26. Geeraedts F, Saluja V, Veer W, Amorij JP, Frijlink HW, Wilschut J, Hinrichs WLJ, Huckriede A. Preservation of the immunogenicity of dry-powder influenza H5N1 whole inactivated virus vaccine at elevated storage temperatures. *AAPS J.* 2010;12(2):215–222.

Table 1: Particle size of nasal powder formulation

The median particle size of each powder formulation, the microcrystalline cellulose, and the trehalose dihydrate used in the present study are listed.

Median Particle Size (Dv50, μm , $n = 3$)

Microcrystalline Cellulose	16.8 \pm 0.1	Trehalose Dihydrate	20.3 \pm 0.4
Nasal Dye Cellulose Powder Formulation	18.1 \pm 0.2	Nasal Dye Trehalose Powder Formulation	16.9 \pm 0.5
Nasal Mn Cellulose Powder Formulation	17.6 \pm 0.5	Nasal Mn Trehalose Powder Formulation	21.6 \pm 2.2
Nasal OVA Cellulose Powder Formulation	18.1 \pm 0.0	Nasal OVA Trehalose Powder Formulation	20.2 \pm 0.7

All data are presented as mean \pm standard deviation.

Table 2: Spray Characteristics of Powder and Liquid Formulation

Formulation	Delivered Weight (%)	Spray Pattern (area, mm ²)	Plume Angle (angle, °)
Nasal Dye Liquid Formulation	101.2 ± 0.5	341.4 ± 8.5	52.3 ± 8.3
Nasal Dye Cellulose Powder Formulation	98.1 ± 2.8	87.3 ± 1.4**	23.3 ± 1.8**
Nasal Dye Trehalose Powder Formulation	99.8 ± 4.3	121.9 ± 14.9**	28.6 ± 0.6**
Nasal Mn Liquid Formulation	101.2 ± 0.5	351.6 ± 20.3	45.1 ± 3.6
Nasal Mn Cellulose Powder Formulation	99.3 ± 1.9	73.3 ± 4.4**	24.0 ± 1.9*
Nasal Mn Trehalose Powder Formulation	99.7 ± 0.6	110.8 ± 4.4**	23.8 ± 5.6*
Nasal OVA Liquid Formulation	100.6 ± 0.6	334.1 ± 8.2	46.9 ± 0.5
Nasal OVA Cellulose Powder Formulation	98.7 ± 0.2	85.3 ± 1.4**	21.9 ± 1.6**
Nasal OVA Trehalose Powder Formulation	98.7 ± 0.3	139.0 ± 1.9**	31.2 ± 5.1*

All data are presented as mean ± standard deviation. * $p < 0.01$, ** $p < 0.001$ vs solution form of each API (t-test).

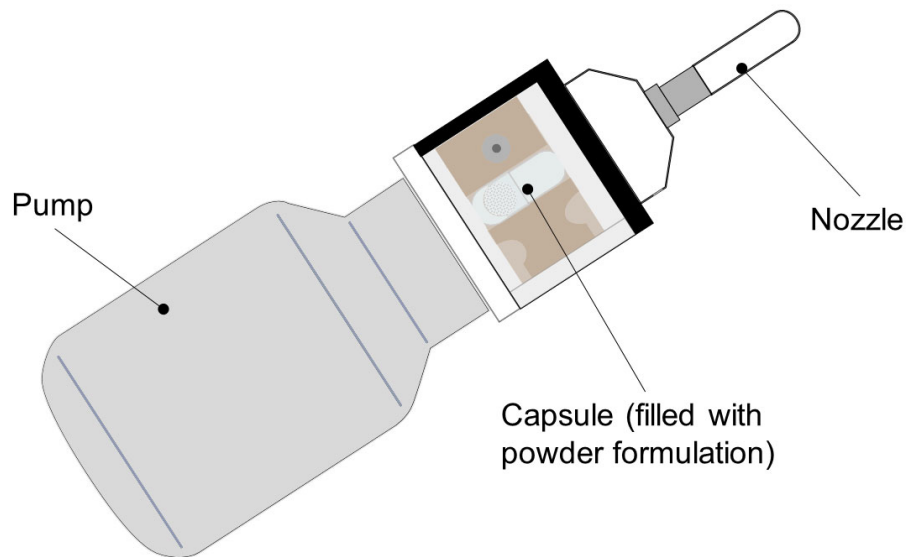


Fig. 1 Nasal delivery device for monkeys (originally developed by Shin Nippon Biomedical Laboratories).

A hydroxypropyl methylcellulose capsule filled with a powder formulation is loaded into the device. After inserting the nozzle into a nostril, the powder formulation is delivered by actuating the pump.

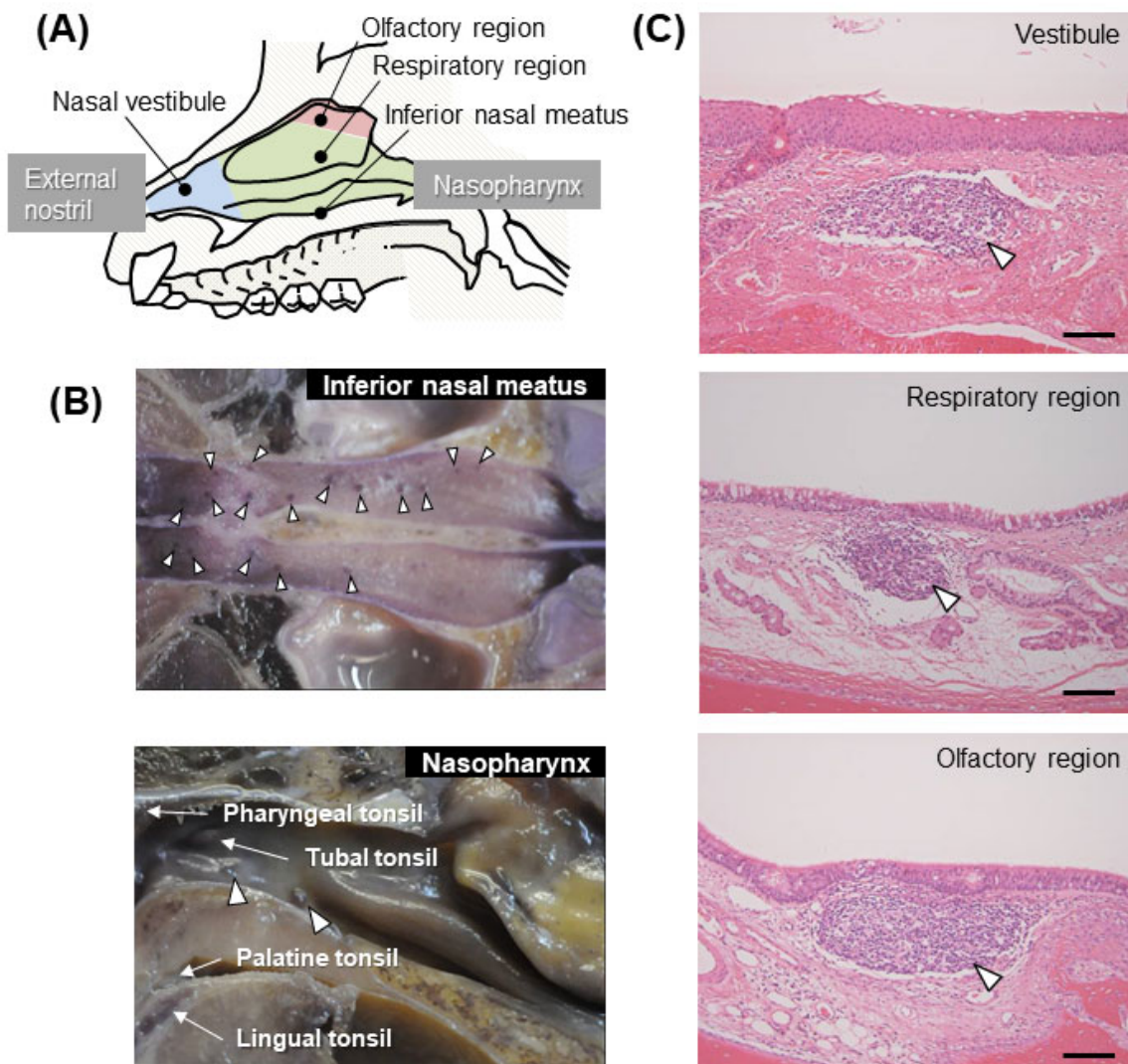


Fig. 2 Localization of nasal lymphatic tissues.

(A) Schematic representation of the nasal cavity in monkeys. (B) Harris hematoxylin staining of inferior nasal meatus and posterior region of the monkey nasal cavity ($n = 1$). (C) HE staining of the nasal vestibule, respiratory region, and olfactory region ($n = 1$). Arrowheads indicate nasopharynx-associated lymphoid tissue. Scale bar = 100 μm .

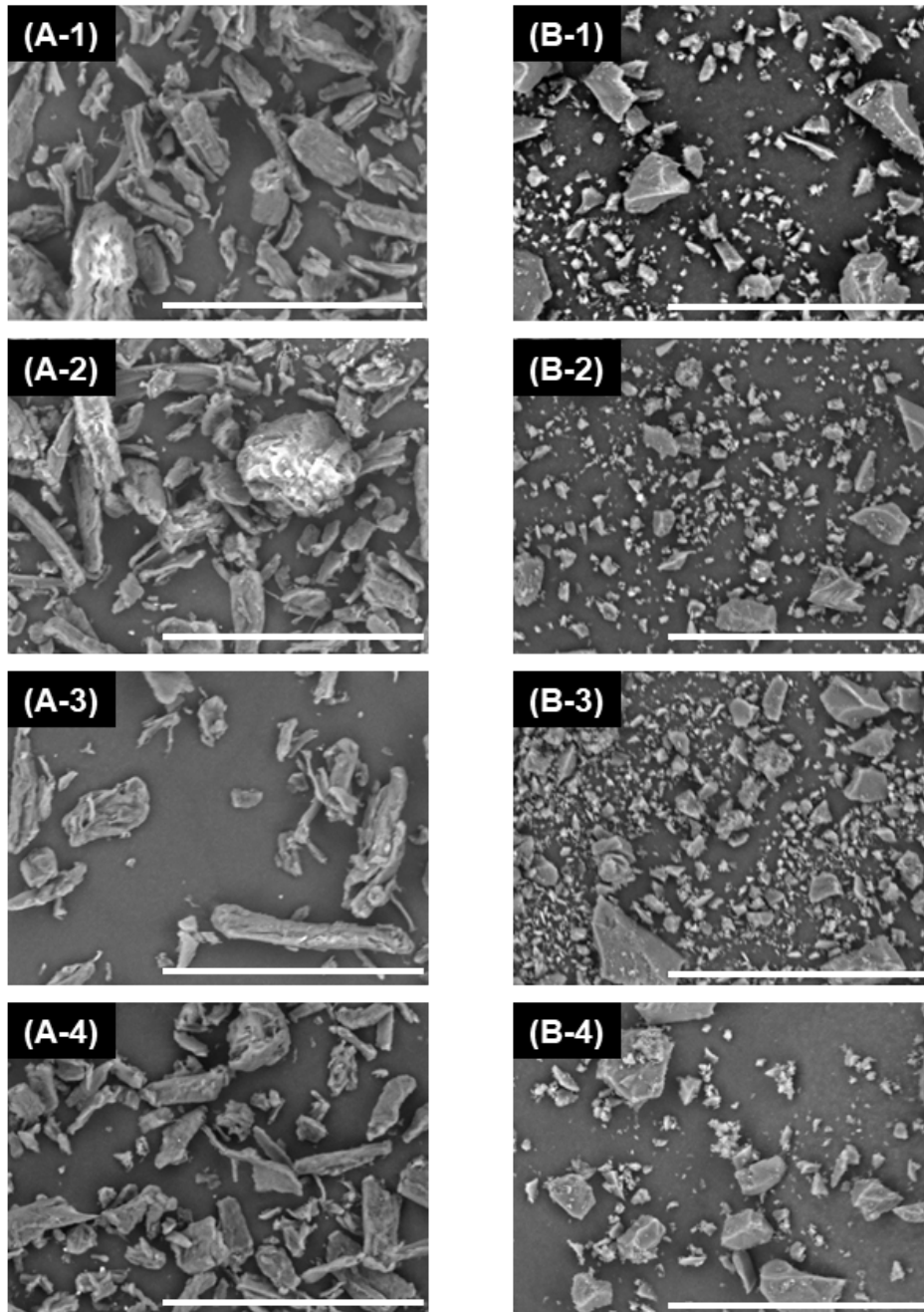


Fig. 3 Scanning electron microscope (SEM) image of nasal powder formulation.

SEM images with magnification of 1000x for each powder formulation, microcrystalline cellulose, and trehalose dihydrate used in the present study were captured. **(A-1)** the microcrystalline cellulose; **(A-2)** Nasal Dye Cellulose Powder Formulation; **(A-3)** Nasal Mn Cellulose Powder Formulation; **(A-4)** Nasal OVA Cellulose Powder Formulation; **(B-1)** the trehalose dihydrate; **(B-2)** Nasal Dye Trehalose Powder Formulation; **(B-3)** Nasal Mn Trehalose Powder Formulation; **(B-4)** Nasal OVA Trehalose Powder Formulation. Scale bar = 100 μm .

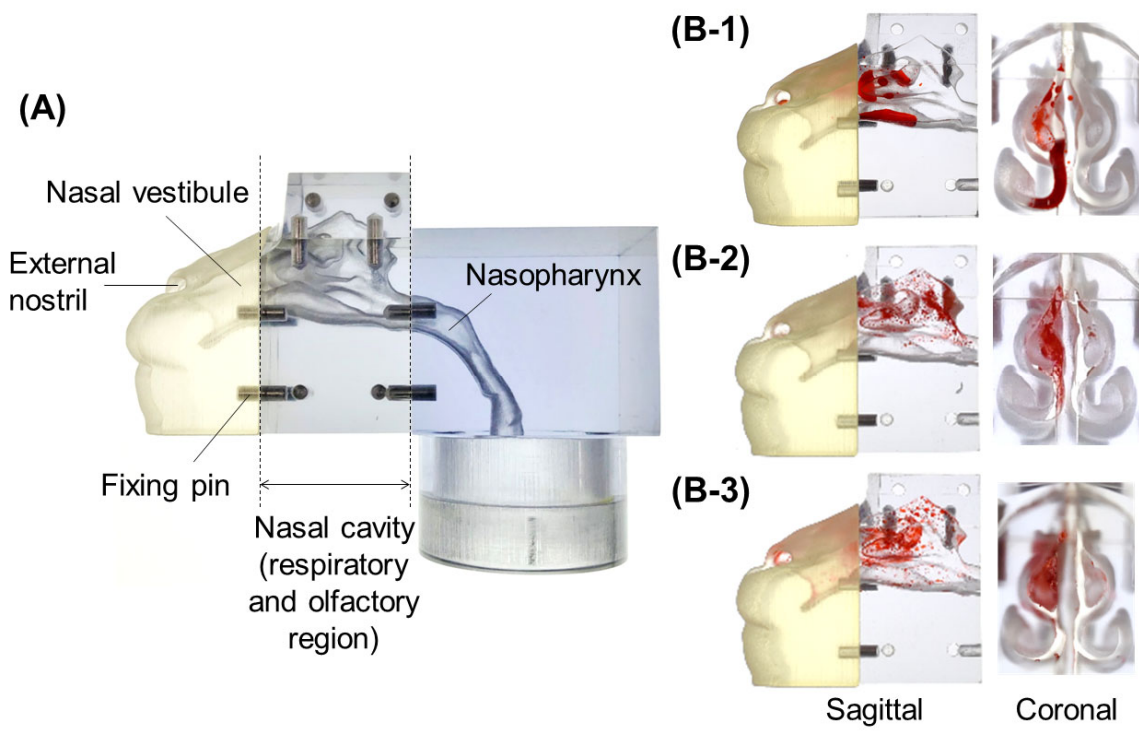


Fig. 4 Distributions of dye delivered into the monkey nasal cavity model.

(A) The nasal cavity model consists of three detachable parts (nasal vestibule, nasal cavity, and nasopharynx). The Nasal Dye Liquid Formulation (B-1), Nasal Dye Cellulose Powder Formulation (B-2), and Nasal Dye Trehalose Powder Formulation (B-3) were administered into the nasal cavity model.

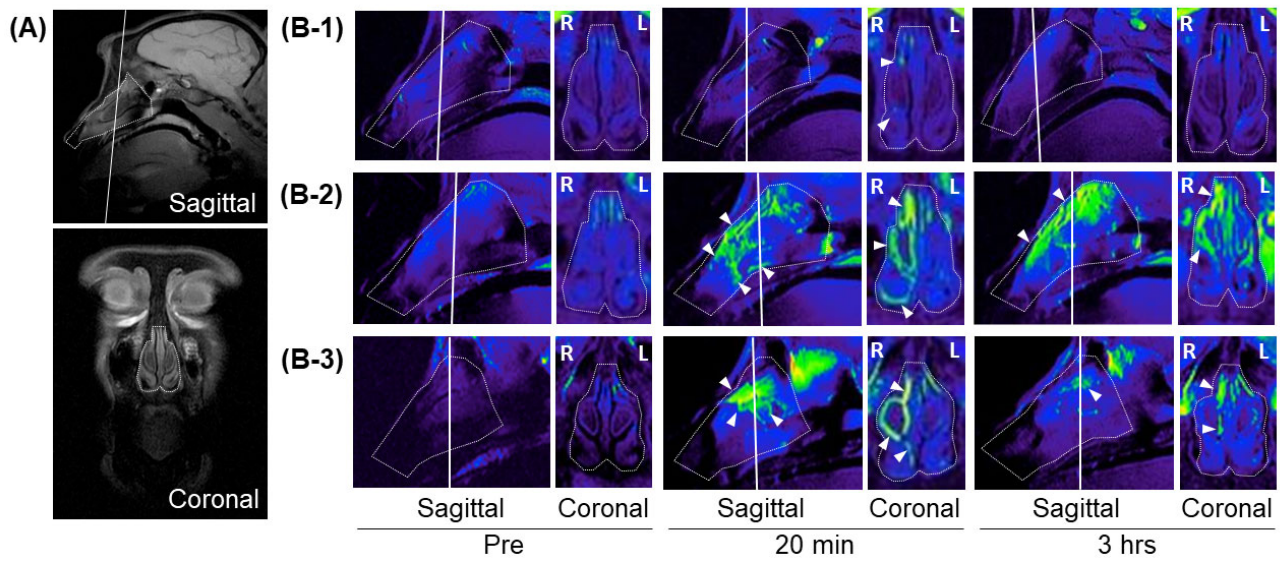


Fig. 5 Images of Mn²⁺ delivered to the monkey nasal cavity using Mn-enhanced MRI.

(A) T1 weighted coronal and sagittal anatomical images of the monkey. Nasal Mn Liquid Formulation (B-1), Nasal Mn Cellulose Powder Formulation (B-2), or Nasal Mn Trehalose Powder Formulation (B-3) was administered intranasally to conscious monkeys. The T1-weighted sagittal and coronal images of the nasal cavity were captured under anesthesia before, and approximately 20 minutes and 3 hours after administration. The white-dotted area shown in both the coronal and sagittal images is the nasal cavity. The white line shown in the sagittal image is the coronal image plane. Arrowheads indicate the localization of the formulation (Mn²⁺ signal as tracer).

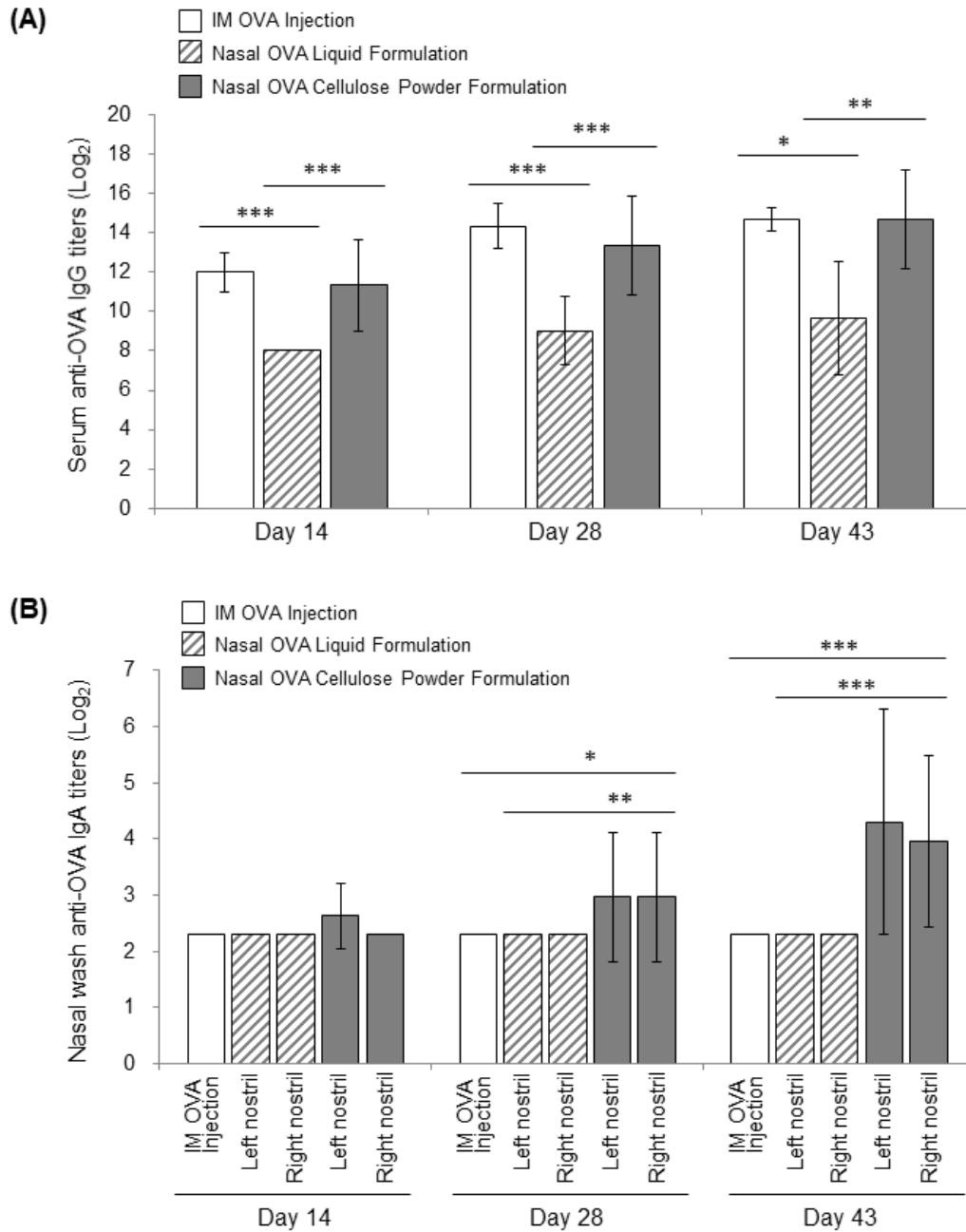


Fig. 6 Serum anti-OVA-IgG antibody titers and nasal wash anti-OVA-IgA antibody titers after immunization with OVA in cynomolgus monkeys.

Monkeys ($n = 3$) were immunized on days 0, 14, and 28 via IM OVA Injection, Nasal OVA Liquid Formulation, or Nasal OVA Cellulose Powder Formulation. The anti-OVA-IgG antibodies in serum samples **(A)** and anti-OVA IgA antibodies in nasal washes **(B)** were measured 14 days after each immunization (mean \pm SD). * $p < 0.05$, ** $p < 0.01$, *** $p < 0.001$